Open access • Journal Article • DOI:10.1109/TSG.2013.2292530

Integrating Electrical Energy Storage Into Coordinated Voltage Control Schemes for Distribution Networks — Source link

Pengfei Wang, Daniel H. Liang, Jialiang Yi, Pádraig Lyons ...+2 more authors

Institutions: Newcastle University, Durham University

Published on: 06 Feb 2014 - IEEE Transactions on Smart Grid (Newcastle University)

Topics: Smart grid and AC power

Integrating Electrical Energy Storage into Coordinated Voltage Control Schemes for Distribution Networks

P. Wang, D. H. Liang, J. Yi, P. F. Lyons, P. J. Davison, P. C. Taylor

***Abstract*-- In this paper, a coordinated voltage control scheme utilizing electrical energy storage (EES) is presented, for future distribution networks with large, clustered distributions of low carbon technologies (LCTs) in terms of both feeder and phase location. The benefits of the EES integrated scheme over conventional voltage control schemes are demonstrated by realizing a set of network scenarios on a case study network both in simulation and in network in the loop (NIL) emulation at a smart grid laboratory facility. The case study uses a rigorously validated model of an actual GB distribution network with multiple EES installations. It was found that the EES integrated voltage control scheme is able to provide increased capability over conventional voltage control schemes and increase the value of EES to network operation.**

***Index Terms*-- Electrical Energy Storage, Coordinated Voltage Control, Network in the Loop Emulation**

I. Nomenclature

Abbreviations

LCT	Low Carbon Technology
PV	Photovoltaic
EV	Electric Vehicle
HP	Heat Pump
DNO	Distribution Network Operator
CLNR	Customer Led Network Revolution
EES	Electrical Energy Storage
OLTC	On Load Tapchanger
MV	Medium Voltage
LV	Low Voltage
FVDF	Feeder Voltage Divergence Factor
VCSF	Voltage Cost Sensitivity Factor
VSF	Voltage Sensitivity Factor
NIL	Network in the Loop
SCADA	Supervision Control and Data Acquisition
SOC	State of Charge
ASHP	Air Source Heat Pump
RTDS	Real Time Digital Simulator
COP	Coefficient of Performance
FACTS	Flexible Alternating Current Transmission System
SVC	Static VAr Compensator
STATCOM	Static Synchronous Compensator

Symbols

$\%VUF$	Percentage voltage unbalance factor
$V_{a,\,b,\,c}$	Three-phase phase voltages (pu)
V_{avg}	Average phase voltage (pu)
$V_{Highest}$	Highest feeder end voltage (pu)
V_{Lowest}	Lowest feeder end voltage (pu)
$C_{P,\,EES}$	Cost of operating EES for one cycle (charge and discharge) (£)
$C_{Capital,\,EES}$	Capital cost of EES (£)
N_{EES}	Total charge and discharge cycles of EES
SOC_T	Target state-of-charge (SOC) of battery (%)
SOC	State-of-charge (SOC) of battery (%)
k_{EES}	EES charging/discharging cost factor
$C_{Q,\,EES}$	Cost of operating the EES reactive power per control cycle (£)
$C_{Capital,\,Inverter}$	Capital cost of inverter system of the EES (£)
$T_{Life,\,span}$	Expected lifespan of inverter (min)
$T_{Control,\,cycle}$	Control cycle (min)
$N_{OLTC,\,Remaining}$	Remaining operation times of the tapchanger
$N_{OLTC,\,Total}$	Estimated total operation times of the tapchanger
$LS_{OLTC,\,Remaining}$	Remaining lifespan of the tapchanger (min)
$LS_{OLTC,\,Total}$	Total lifespan of the tapchanger (min)
C_{OLTC}	Cost of OLTC tap operation (£)
$C_{OLTC,\,Replacement}$	Capital cost of replacing the tapchanger (£)
$VCSF_{ij}$	VCSF of control device j with respect to node i (pu/£)
C_j	Cost of operating control device j to achieve voltage change ΔV_{ij} at node i (£)
ΔV_{ij}	Voltage change at node i due to the operation of control device j (pu)
ΔV_{isoln}	Voltage change at node i due to the deployment of voltage control solution (pu)
ΔV_i	Original voltage execution at node i (pu)
$\Delta V'_i$	Updated voltage execution at node i (pu)

This work was supported in part by the Office of the Gas and Electricity Markets under Low Carbon Network Fund.

P. Wang, J. Yi, P. F. Lyons, P. J. Davison and P. C. Taylor are with the School of Electrical and Electronic Engineering, Newcastle University, Newcastle upon Tyne, NE1 7RU, UK (e-mail: p.wang5@ncl.ac.uk). D. H. Liang is with the School of Engineering and Computer Science, Durham University.

ΔP_{EES}	Required real power change from EES (kW)
ΔQ_{EES}	Required reactive power change from EES (kVAr)
$\Delta V_{i,\ required}$	Required voltage change at node *i* (pu)
$VSF_{i\_P,\ EES}$	VSF of node *i* for the real power of EES (pu/kW)
$VSF_{i\_Q,\ EES}$	VSF of node *i* for the reactive power of EES (pu/kVAr)

II. Introduction

The projected proliferation of Low Carbon Technologies (LCTs), such as wind generation, Photovoltaic (PV) generation, Electric Vehicles (EVs) and heat pumps (HPs), is anticipated to result in a paradigm shift in the use of electricity in distribution networks. This will in turn bring new challenges for distribution network operators (DNOs). This paper describes work being undertaken as part of the Customer Led Network Revolution (CLNR) project, funded by the UK regulator (Ofgem). A key objective of this project is to investigate how smart grid interventions such as Electrical Energy Storage (EES) and coordinated control systems can be used to facilitate the connection of LCTs in distribution networks. As part of the CLNR project, six EES units will be installed at various voltage levels and locations, with rated powers varying from 50kW to 2.5MW on three test networks. Additionally a hierarchical control system, currently in development, will also be deployed to enable evaluation of the operation of EES in an integrated control system.

In this paper, a coordinated voltage control scheme integrating EES units of various ratings, capacities and locations is presented. The proposed voltage control scheme can coordinate the operation of on load tapchangers (OLTC) not only at primary substations but also at secondary substations, as well as EES units at medium voltage (MV) remote feeder ends and at the low voltage (LV) remote feeder ends [1], [2]. In addition, feeder voltage divergence factor (FVDF) and percentage voltage unbalance factor (%VUF) are utilized as network voltage metrics for networks with large, clustered distributions of LCT. Voltage cost sensitivity factor (VCSF) is defined to represent how cost effective each network intervention is, in terms of voltage control. Voltage sensitivity factor (VSF) is used to determine the required response from each network intervention. These metrics and factors are then used in the proposed control scheme to fully realize the capabilities of EES in the system.

This proposed control scheme is evaluated with a real, smart grid enabled case study network. Multiple LCT clusters are connected to both the 20kV MV feeders and the 0.4kV LV feeders of the case study network, to create a future scenario. Simulation and Network in the Loop (NIL) emulation are utilized to test the operation of the proposed control scheme. It was found that the proposed coordinated voltage control scheme integrating EESs is particularly appropriate for future distribution networks with highly uneven distributions of load and generation.

The rest of this paper is organized as follows. In section III, a summary of literature relating to the voltage problems arising from large, clustered distributions of LCTs is introduced. This is followed by a review of previous research on EES for voltage control, collaborative voltage control schemes in distribution networks, voltage imbalance and control. In section IV, the proposed voltage control scheme is presented. In section V, a case study network and the implementation of the proposed control scheme in the case study network are introduced. In section VI, the simulation and evaluation results from the application of the control scheme in the case study are presented. In section VII, the conclusions are drawn.

III. Background

A. Voltage Issues in Future Distribution Networks

In the UK, steady-state voltages should be maintained within ±6% of the nominal voltage in the systems above 1kV and below 132kV, and between +10% and -6% of the nominal voltage in 0.4kV, LV networks [3].

Wind generation with installed capacity at MW level forms the largest renewable part of the UK generation portfolio. Much of this is connected to weak, rural distribution networks, which are susceptible to voltage rise issues [4]. Similarly, large concentrations of microgeneration, such as domestic PV generation clusters, can cause voltage rise issues on LV networks [5], [6]. Conversely, large concentrations of load LCTs, such as EV and HP, will result in undervoltage issues [7], [8].

Furthermore, as these distributions and clusters of LCTs are predominantly unplanned, distribution networks are likely to experience both violations of upper and lower voltage limits simultaneously on separate MV or LV feeders. Common mode voltage solutions such as OLTC equipped transformers, are often used to resolve steady-state voltage issues, may not be capable of adequately resolving this scenario as they increase or decrease voltage across the entire network they supply.

B. EES for Voltage Control

A comprehensive review of the possible benefits of EES has been presented previously [9]. EES can be utilized to support a heavily loaded feeder, provide power factor correction, reduce the need to constrain DG, minimize OLTC operations and mitigate flicker, sags and swells [9].

EES is shown to voltage regulation through reactive power support, frequency response and power factor correction in [10]. A distribution network voltage support operation strategy for EES has been proposed that operates the EES to export real and reactive power with reactive power priority [11]. The export of real and reactive power from the EES is optimized for voltage control by utilizing the ratio of voltage sensitivities of real and reactive power export, so that the size of the EES unit can be minimized. EES is used locally to mitigate the voltage rise due to a windfarm by absorbing reactive power in [12]. The voltage changes, to accommodate the wind

generation, with and without reactive power compensation, at 12 LV nearby busbars were calculated. The lifetime costs associated with the EES, cognizant of the power rating and energy capacity of the devices, were then compared. Three control strategies for dispersed flow batteries have been previously reported and compared for voltage regulation in distribution networks with high PV penetration [13].

In [14], an optimal battery EES operation strategy with other voltage control techniques for loss reduction and voltage control has been proposed. A Tabu search algorithm is employed to search the optimal schedule at 30 minute intervals to build a control reference for the daily EES operation. The optimal operation schedule of EES achieved can realize voltage control and network loss reduction. However, 30-minute time intervals may not be sufficient for real time voltage control in distribution networks. A coordinated voltage control scheme including EES, OLTC and voltage regulators is presented to mitigate voltage rise problem caused by high PV penetration in [15]. Multiple benefits can be achieved, such as reducing the switching operation times of existing voltage control devices, and reducing network losses. However, in this paper only the active power of EES is controlled.

In [16], it has been found that unbalanced three-phase control of the EES, can mitigate voltage rise due to PV generation more efficiently than the conventional, balanced three-phase control.

C. Current and Emerging Coordinated Voltage Control Schemes in Distribution Networks

Conventional distribution networks already adopt a number of locally controlled voltage control devices, such as primary OLTC and flexible alternating current transmission system (FACTS), which includes static VAr compensators (SVCs) and static synchronous compensators (STATCOMs) [17]. Currently, the voltage control devices are locally controlled to achieve a passive coordinated voltage control scheme in distribution networks [18]. This passive coordinated voltage control scheme is adequate for most cases in current distribution networks. However, to facilitate the anticipated growth of LCTs, the existing control approach may not be sufficient.

It should be noted here that EES can be considered to be a FACTS device with a large real power storage capability, or an additional type of FACTS device. In addition to reactive power support the EES is also able to provide substantial real power support to these networks. The capability to supply real power support is important in distribution networks, due to their low X/R ratios. It can be seen therefore that reactive power control in distribution networks is less efficient than that in transmission networks [19]. Furthermore, use of reactive power control only may cause larger power flows, which can increase network losses. In this work FACTS devices are not specifically discussed however it is easy to integrate other FACTS devices into the scheme proposed in this paper, by considering them as an EES without a real power import/export capability.

Previous research has reported a number of coordinated voltage control approaches for future distribution networks, primarily to improve network performance [20] and facilitate the connection of LCTs [21].

Optimized, coordinated voltage control schemes with heuristic or meta-heuristic algorithms have been reported in previous research [22], [23]. The voltage control problem is formulated into a mathematical optimization problem by defining the control objectives and constraints. The control objectives can include reducing network losses and flattening the voltage profiles, while the constraints can cover the voltage and thermal limits in the network. The formulated optimization problem is solved with heuristic or meta-heuristic algorithms, such as generic algorithms [22] and evolutionary particle swarm optimization algorithms [23]. In these control schemes, network model based online load flow analysis is required to find the optimized solution.

Database driven control strategies have also been shown previously to have an application in coordinated voltage control schemes [24], [25]. In these schemes, the solution of the coordinated voltage control is 'learned' from a database, which contains control solutions from historical operation or from previously completed offline studies. The implementation of the database can improve overall controller performance and avoid the risks of non-convergence. However, a solution database, developed from offline analysis, and intelligent database self-learning algorithms are needed.

All the voltage control schemes discussed above need on-line load flow engine and/or solution database. In most of these control schemes, only the steady-state voltage problems at MV voltage level are considered. The steady-state voltage problems at the LV voltage level and voltage imbalance problems are not considered.

D. Voltage Imbalance and Control

The consumer driven and non-centrally planned growth of single-phase connected LCTs, such as EVs and domestic PVs, may also result in unbalanced voltages on LV distribution networks [26], [27].

Voltage imbalance is a condition in which the three-phase voltages differ in amplitude or are displaced from their normal 120° phase relationship or both. Conventionally, the uneven distribution of single-phase loads is the major cause of voltage imbalance [28]. Single-phase generation LCTs can also result in unbalanced voltages [26], [27]. The %VUF in distribution networks in the UK [29] and Europe [30] is used to define the acceptable level of voltage imbalance in a system. A number of definitions exist and in this work a definition from [31] is used, as shown in (1).

$$\%VUF = \frac{Max\left|V_{a,b,c} - V_{avg}\right|}{V_{avg}} \times 100\% \quad (1)$$

Where:

%VUF Percentage voltage unbalance factor

$V_{a,b,c}$ Three-phase phase voltages (pu)

V_{avg} Average phase voltage (pu)

The %VUF has a regulatory limit of 1.3% in the UK, although short-term deviations (less than 1 minute) may be allowed up to 2%, which is the standard limit used for the maximum steady-state %VUF allowed in European networks [29], [30].

Network reconfiguration and reinforcement can be used to solve voltage imbalance problems. Additionally, specially designed STATCOMs and other power electronics devices could provide the functionality to compensate for unbalanced voltages in LV distribution systems [28].

It is worth noting that voltage rise has been previously determined to be the first technical constraint to be encountered as penetrations of microgeneration increase [27]. However, it is anticipated that voltage imbalance may also become a constraint as secondary OLTCs, which can mitigate overvoltage on LV systems [32], are unable to reduce the voltage imbalance on these networks due to the growth of clusters of load and generation LCTs.

In this work, the proposed coordinated voltage control scheme, integrates the control of the primary and secondary transformer OLTCs and EES units located at different voltage levels.

This control scheme provides a cost-optimized voltage control solution for the distribution networks with both generation LCTs and load LCTs. Additionally, this coordinated voltage control approach provides a holistic solution not only to steady-state voltage problems on MV and LV networks but also to voltage imbalance in LV networks.

IV. Coordinated Voltage Control System

A. Voltage Control Scheme Objective

The previous sections detailed the voltage issues that are expected to arise in future distribution networks due to the increased possibilities of clusters of load and generation LCTs, in terms of both feeder and phase location. It was seen that conventional primary transformer tapchanger based voltage control schemes may not be able to provide a technical solution due to the common mode nature of their control interventions. In contrast, many coordinated voltage control schemes require complex on-line load flow analysis based on detailed network models, which need to be continually updated, to determine control solutions.

The control scheme in this work has been designed to be robust and is not reliant on artificial intelligence techniques or complex network models to select cost-optimized, coordinated solutions to solve steady-state voltage problems by controlling OLTCs and EES units.

This proposed control scheme does not require online load flow analysis. Instead, voltage cost sensitivity factors and voltage sensitivity factors, calculated with offline load flow analysis, are used to find the cost-optimized control solution and to determine the response required from each solution. FVDF has been defined to represent the network feeder voltage divergence. FVDF and %VUF are used to represent the divergence and imbalance, caused by loads, generations and clusters of LCTs, on feeders and phases. These factors are used to determine whether common mode voltage solutions are appropriate to resolve the voltage issues that have been identified by the scheme.

B. Feeder Voltage Divergence Factor

FVDF is defined as the maximum feeder voltage divergence among voltages (pu value) at the remote ends of different feeders downstream of a common mode controlled busbar, as expressed in (2):

$$FVDF = V_{Highest} - V_{Lowest} \tag{2}$$

Where:

$V_{Highest}$ Highest feeder end voltage (pu)

V_{Lowest} Lowest feeder end voltage (pu)

As illustrated in Fig. 1, the threshold of FVDF is determined using the statutory voltage limits, the maximum voltage variation at the remote ends of the feeders following the upstream tapchanger tap operation and the maximum voltage change at the remote ends of the feeders in a control cycle due to load or generation change. These maximum voltage changes can be derived from offline load flow analysis.

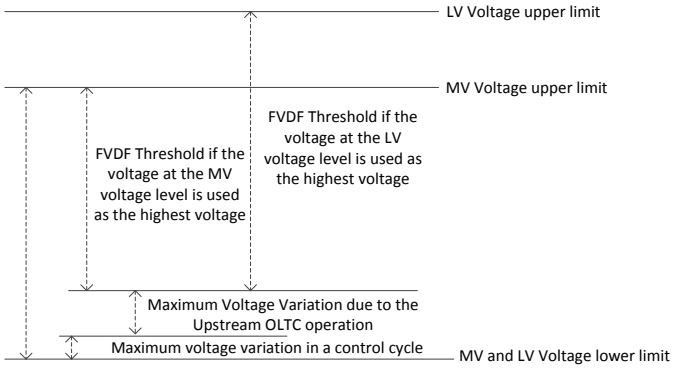

Fig. 1 FVDF threshold determination

C. Voltage Sensitivity Factor

1) Electrical Energy Storage

For the EES, voltage sensitivity factors describe the sensitivities of network voltages to the real power P and reactive power Q injections from the EES, which can be analyzed through the use of the Jacobian Matrix [33], as shown in (3):

$$\begin{bmatrix} \Delta\boldsymbol{\theta} \\ \Delta\mathbf{V} \end{bmatrix} = J^{-1}\begin{bmatrix} \Delta\mathbf{P} \\ \Delta\mathbf{Q} \end{bmatrix} = \begin{bmatrix} \frac{\partial\boldsymbol{\theta}}{\partial\mathbf{P}} & \frac{\partial\boldsymbol{\theta}}{\partial\mathbf{Q}} \\ \frac{\partial\mathbf{V}}{\partial\mathbf{P}} & \frac{\partial\mathbf{V}}{\partial\mathbf{Q}} \end{bmatrix} \times \begin{bmatrix} \Delta\mathbf{P} \\ \Delta\mathbf{Q} \end{bmatrix} \tag{3}$$

Voltage sensitivity factors relate the change in voltage at a network node due to a change in real or reactive power at a

particular load or generation node elsewhere in the network. A large voltage sensitivity factor indicates that a variation in nodal real or reactive power leads to a large change in voltage at a specified network location.

2) On Load Tapchanger (OLTC)

The network voltage changes arising from single tap operation of a tapchanger are defined as voltage sensitivity factors of the tapchanger in this paper. The voltage sensitivity factor of a single tap operation depends on multiple parameters, such as the voltage at the primary side, load condition, and the tapchanger position. It has been demonstrated by simulation that the tap position of the tapchanger has a much larger effect on the voltage sensitivity factors of a tapchanger than the other parameters. Thus, a lookup table of voltage sensitivity factor based on the tapchanger tap position is used in this voltage control scheme.

D. Cost Functions

1) Electrical Energy Storage

Here, the cost of the EES is defined by the capital investment and the cost related to the state of charge (SOC). EES has a time limit if the real power is used for voltage control, due to the finite energy capacity of the energy storage. A target SOC is defined for future application and other functions. Therefore, the cost of the real power for the EES can be calculated from (4):

$$C_{P,EES} = \frac{C_{Capital,EES}}{N_{EES}} + k_{EES} \times \left(SOC_T - SOC \right) \tag{4}$$

Where:

$C_{P,EES}$ Cost of operating EES for one cycle (charge and discharge) (£)

$C_{Capital,EES}$ Capital cost of EES (£)

N_{EES} Total charge and discharge cycles of EES

SOC_T Target state-of-charge (SOC) of battery (%)

SOC State-of-charge (SOC) of battery (%)

k_{EES} A factor relating the deviation of SOC from the target SOC to the cost of charging/discharging the EES. The cost becomes larger when the SOC approaches 100% during charging of the EES and also when the SOC approaches 0% during discharging

Thus, the cost function for real power in an EES is a combination of capital investment and an offset to account for a changing SOC. It is assumed that the net power consumption of the EES is zero and that the cost of exporting and importing are equal.

An approximate cost function for the cost of using the reactive power capability of the EES is defined as:

$$C_{Q,EES} = \frac{T_{Control\ cycle}}{T_{Lifespan}} \times C_{Capital,\ Inverter} \tag{5}$$

Where:

$C_{Q,EES}$ Cost of operating the EES reactive power for control cycle (£)

$C_{Capital,\ Inverter}$ Capital cost of inverter system of the EES (£)

$T_{Lifespan}$ Expected lifespan of inverter (min)

$T_{Control\ cycle}$ Control cycle (min)

It should be noted that the EES is a multifunction network intervention, which means it may not only be used for voltage control. The other functions, such as power flow management, should also be considered when evaluating the capability of EES to contribute to the network operation in distribution network control systems.

2) On Load Tapchanger (OLTC)

The cost of primary tapchanger operation is calculated based on the total and remaining lifespan of the tapchanger equipped transformer, the estimated lifetime number of operations and the total cost of replacing the OLTC transformer. The remaining number of tapchange operations is defined to be a function of the remaining and total lifespan of the transformer and the estimated total number of tapchange operations:

$$N_{\text{OLTC, Remaining}} = \frac{LS_{\text{OLTC, Remaining}}}{LS_{\text{OLTC, Total}}} \times N_{\text{OLTC, Total}} \tag{6}$$

Where:

$N_{\text{OLTC, Remaining}}$ Remaining operation times of the tapchanger

$N_{\text{OLTC, Total}}$ Estimated total operation times of the tapchanger

$LS_{\text{OLTC, Remaining}}$ Remaining lifespan of the tapchanger (min)

$LS_{\text{OLTC, Total}}$ Total lifespan of the tapchanger (min)

The cost of each OLTC tap operation is given in (7):

$$C_{\text{OLTC}} = \frac{C_{\text{OLTC Replacement}}}{N_{\text{OLTC, Remaining}}} \tag{7}$$

Where:

C_{OLTC} Cost of OLTC tap operation (£)

$C_{\text{OLTC Replacement}}$ Cost of replacing the tapchanger (£)

E. Voltage-cost sensitivity factor (VCSF)

VCSF is used to account for the cost associated with the utilization or deployment of a network solution within the proposed control algorithm.

The VCSF is derived as a function of the voltage sensitivities and network intervention operating costs. For example, the VCSF of device j to node i, $VCSF_{ij}$ is defined as:

$$VCSF_{ij} = \frac{\Delta V_{ij}}{C_j} \tag{8}$$

Where $VCSF_{ij}$ quantifies the voltage change ΔV_{ij} at node i with a cost of C_j to operate device j to achieve the voltage change ΔV_{ij} at node i.

F. Control Flow Chart

The flow chart of the proposed control scheme is illustrated in Fig. 2. The following sections describe in further detail the operation of each of the phases of the coordinated voltage control scheme.

Phase A: Key locations or 'critical nodes' have been identified using offline load flow analysis utilizing the network model and data. These critical voltage nodes of the network are continuously monitored. A set of N critical nodes, where sustained voltage problems occur, are identified in this phase.

Phase B: The voltage problems at each of the N nodes identified in the previous phase are classified as per Table I.

TABLE I
VOLTAGE PROBLEM CLASSIFICATION

Node	***i***
Steady-state voltage excursion	None/Overvoltage/Undervoltage
FVDF > Threshold	Yes/No
%VUF > Regulatory Limit	Yes/No

Phase C: The cost-optimized voltage control solutions for voltage problems at each node are identified in this phase. The solutions available to solve each of these problems are determined using the classifications defined in the previous phase. The required response from the network solution is determined using voltage sensitivity factors.

For example, if a sustained overvoltage has been detected at node i and the FVDF is above the threshold, the set of network solutions available are defined to be those that are located on the feeders with the highest and lowest voltages fed from the common mode controlled busbar. The solution with the largest VSCF in this set will be selected to decrease the FVDF within the threshold. Voltage sensitivity factors will be used to compute the required response from the networks solution to reduce the FVDF.

The change in the voltage ΔV_{isoln} , due to the deployment of the FVDF solution is computed, using voltage sensitivity factors, and is added arithmetically to the voltage excursion ΔV_i to give $\Delta V_i^{'}$. The network solution with the largest VCSF is selected to mitigate the overvoltage. Voltage sensitivity factor is again used to calculate the required response from the second network solution deployed which would reduce $\Delta V_i^{'}$ to zero. If more than one solution is required then the solution available with the next highest VCSF is also selected and the required response calculated using voltage sensitivity factors.

Phase D: Deploy voltage control solutions for the set of N nodes.

This voltage control scheme has been designed to be particularly appropriate for networks with large, clustered distributions of LCTs, in terms of feeder and phase location. Moreover, it is likely that these clusters are to be more prevalent, especially in liberalized, unbundled electricity markets, due to the consumer-driven and non-centrally planned connection of LCTs.

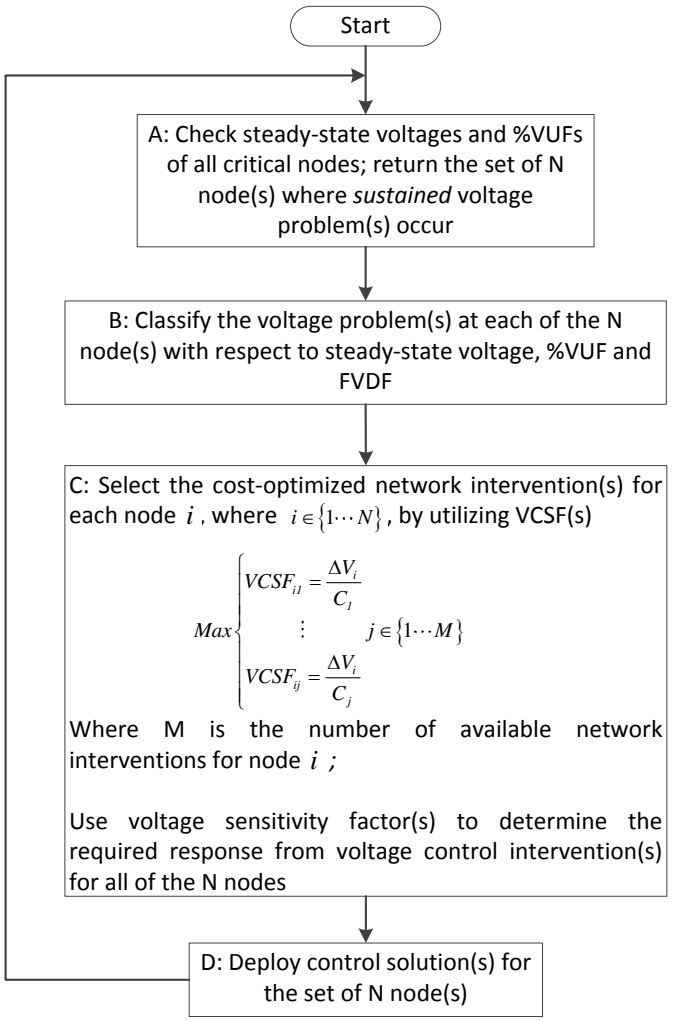

Fig. 2 Flow chart of proposed voltage control scheme

G. EES Control and OLTC Control

Both real power and reactive power of EES can be controlled. Here the real power and reactive power are selected as per the VCSFs, which are based on charging/discharging command, the SOC and the predefined target SOC.

The import/export power change of the EES required is determined with the VSF by (9) and (10).

$$\Delta P_{EES} = (\Delta V_{i,required}) / VSF_{i\_P,EES} \tag{9}$$

$$\Delta Q_{EES} = (\Delta V_{i,required}) / VSF_{i\_Q,EES} \tag{10}$$

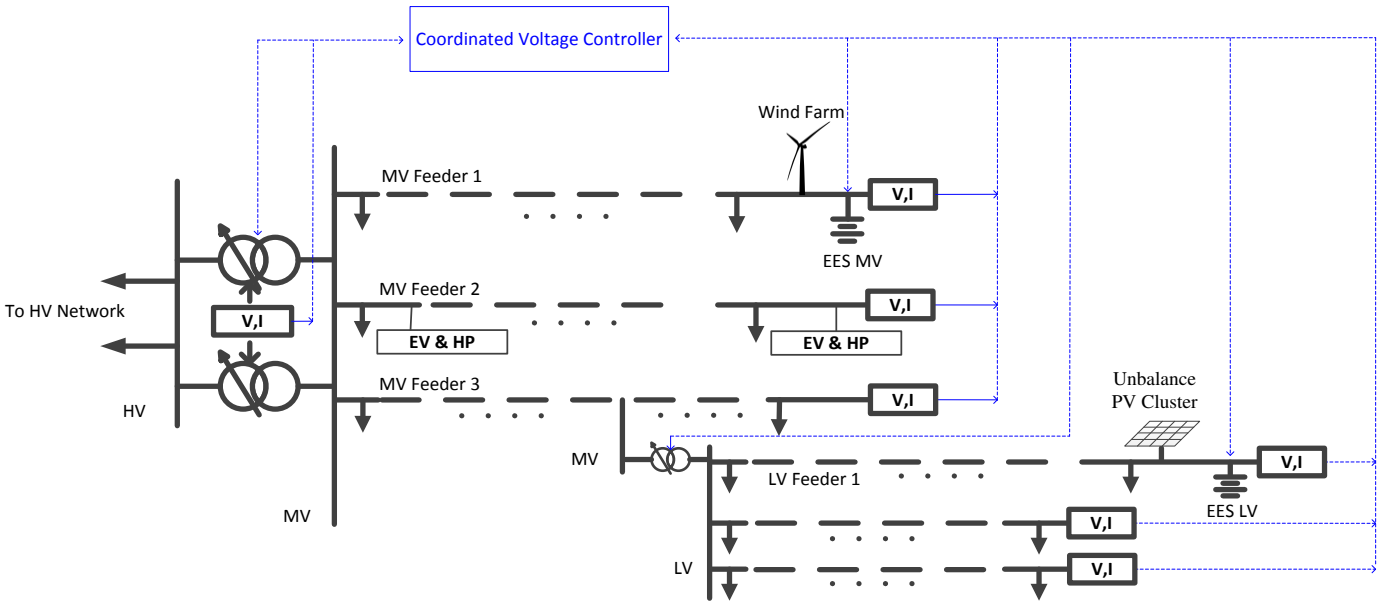

Fig. 3 Case study network and coordinated voltage control scheme

where:

ΔP_{EES} : Required real power change from EES (kW)

ΔQ_{EES} : Required reactive power change from EES (kVAr)

$\Delta V_{i,required}$: Required voltage change at node *i* (pu)

$VSF_{i\_P,EES}$: Voltage sensitivity factor of node *i* for the real power of EES (pu/kW)

$VSF_{i\_Q,EES}$: Voltage sensitivity factor of node *i* for the reactive power of EES (pu/kVAr)

Similarly, the tapchanger is controlled based on the magnitude of voltage excursion and the VSFs of the tapchanger.

V. Case Study

A. Case Study Network

A rural network, which is located in the northeast of England, and owned by Northern Powergrid, is adopted as the case study network to evaluate the proposed control scheme. A single line diagram of this case study network is illustrated in Fig. 3.

In order to apply a future scenario to the case study network, a 5MW windfarm has been connected to MV Feeder 1, while a 10% domestic penetration rate of EVs and air source heat pumps (ASHPs) has been evenly distributed along MV Feeder 2. Furthermore, it has been assumed that a PV cluster has been developed on LV Feeder 1, which is one of the LV network feeders connected to MV Feeder 3. The distribution of PV generations across this cluster is uneven across the phases of the feeder. Specifically, PV penetration rates of 38%, 77% and 33% are used for phase A, B and C respectively.

Furthermore, demand profiles of each MV feeder, windfarm generation data, profiles of domestic load and multiple domestic LCTs are used to create the future scenario.

B. Windfarm Generation Profile and Demand Profile

Wind data from 30 windfarms connected to the Northern Powergrid distribution network have been analyzed to generate a set of windfarm daily profiles for this work. A typical daily generation profile for the windfarm connected to MV Feeder 1 is derived from this data, as illustrated in Fig. 4.

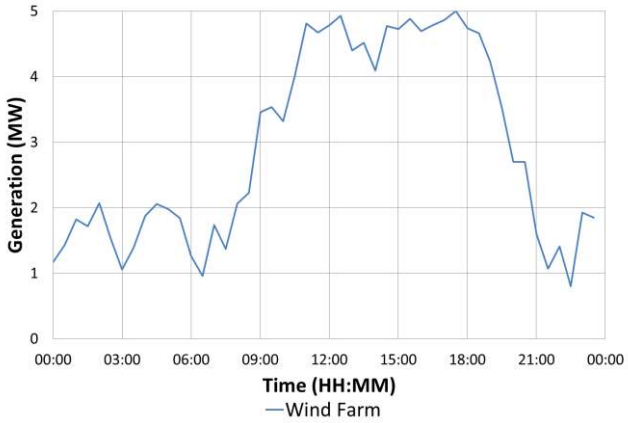

Fig. 4 Daily generation profile of a 5MW windfarm

Typical daily demand profiles, from SCADA data on the case study network, of the MV feeders are illustrated in Fig. 5.

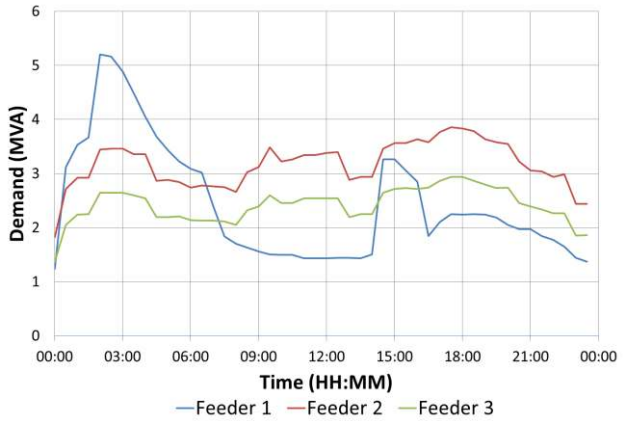

Fig. 5. Demand profiles of MV feeders

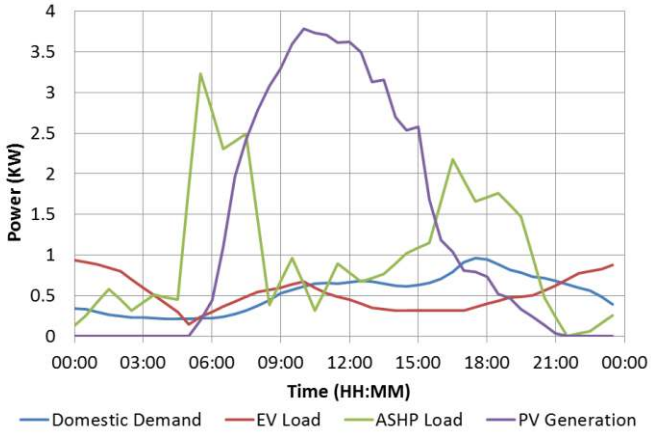

Fig. 6. Profiles of domestic demand, EV, ASHP and PV

It can be seen from Fig. 5 that there are already significant differences between the demands of the three MV feeders, especially between the demand of MV Feeder 1 and that of MV Feeder 2. This is due to the distribution of customers supplied by each feeder. The customer details of each MV feeder are shown in Table II. It can be seen that 90% of the customers on MV Feeder 1 are domestic customers, and 47% of these domestic customers are Super Tariff Customers. Super Tariff, which gives cheap-rate electricity for 5-6 hours overnight and 2 hours at lunchtime, is popular with customers in the case study area due to the prevalence of electric storage heating.

TABLE II
CUSTOMER DETAILS

MV Feeder	Domestic Customer (%)	Super Tariff Domestic Customer (%)
Feeder 1	90.00%	46.86%
Feeder 2	76.24%	24.68%
Feeder 3	84.59%	26.38%

C. Smart Meter Surveys and Profile Development

Historical data from over 5000 domestic customers, covering the period May 2011 to May 2012 was used to derive typical domestic profiles in the CLNR project. A typical domestic demand profile is used here, as shown in Fig. 6.

The PV generation profile, load profiles of electrical vehicles and heat pumps are also shown in Fig. 6. The PV generation profile is derived from disaggregated enhanced metering data available from CLNR project. The electrical profiles of ASHPs in detached and semi-detached houses are generated based on the thermal profiles, which are derived and aggregated in previous work [34]. A coefficient of performance (COP) value of 2.5 has been assumed. This value has been selected to be in the middle of the range of COP values (2-3) found in earlier work [7], [35] and [36]. The EV consumer model used in this work was based on profiles developed and reported previously [37].

D. Control Scheme Implementation

As shown in Fig. 3, the coordinated voltage controller monitors the voltage at the ends of MV feeders and critical LV feeders, and sends control commands to network interventions. In this case study, the network solutions include the tapchanger located at the primary substation and the secondary substation to which the PV cluster is connected, as well as the EES units located at the end of MV Feeder 1 and at the end of LV Feeder 1, MV EES and LV EES respectively. The rated power and capacity are 2.5MW and 5MWh for MV EES, and 0.05MW and 0.1MWh for LV EES. It should be noted here that the maximum reactive power of each EES is 0.8 times of the rated power, as per the units to be installed for the CLNR project.

The VSFs of the EESs and tapchangers were calculated by running an offline load flow analysis on a validated network model. The VSFs for critical nodes due to the operation of multiple network interventions are expressed in Table III. The VSFs of EES are expressed in 1×10^{-3} pu / 50kVA . The VSFs of tapchangers are expressed in 1×10^{-3} pu / tap step and is calculated by increasing one tap step from the middle tap position.

TABLE III
VOLTAGE SENSITIVITY FACTORS OF EES AND TAPCHANGER (1×10^{-3} pu/50kVA or 1×10^{-3} pu/tap step)

	MV Feeder 1 End	MV Feeder 2 End	LV Feeder 1 End
MV EES	1.092	0.110	0.115
LV EES	0.106	0.106	36.577
Primary tapchanger	15.000	15.700	16.900
Secondary tapchanger	N/A	N/A	21.300

The cost of different network interventions are calculated based on the real information from the case study network, with the approach specified in previous sections.

In this case study network, the transformers at the primary substation have been in service for 46 years since their installation in 1966. Therefore, the estimated remaining number of tapchange operations is substantially less than that of the new on load tapchanger transformer, which has been

recently installed at the secondary substation. In this paper, it is assumed that the lifespan and the total estimated number of tapchange operations of each transformer are 50 years and 80,000 times, respectively. Furthermore, the indicative cost of replacing the current primary on load tapchanger equipped transformer is composed of the capital costs of two transformers and all other enabling works, including the costs of civil, installation, commission and protection. The cost of replacing the secondary transformer tapchanger is assumed to be its capital investment.

The capital investment and total charge discharge cycle are also from the CLNR project.

Therefore, the cost of operating EES and using the tapchanger are detailed in Table IV. The cost of EES is based on 50kVA and at target SOC.

TABLE IV
COST OF EES (£/50kVA) AND TAPCHANGER (£/tap step operation)

	Cost
MV EES	18.31
LV EES	102.90
Primary tapchanger	218.75
Secondary tapchanger	0.33

It can be seen from Table IV that the cost per kW of the MV EES is much smaller than that of the LV EES. That is because the cost per kW of the EES is decreasing with the increasing size. It can also be found that the cost per operation of the primary tapchanger is much greater than that of the secondary tapchanger. This is due to the primary tapchanger being in service for 46 years, while the secondary tapchanger has been recently installed, therefore the secondary tapchanger has larger numbers of tap change operations remaining than the primary tapchanger. Additionally, the capital cost of the primary transformer tapchanger is much greater than that of the secondary tapchanger.

The VCSFs in this case study were calculated using (8) and the values in Table III and Table IV. The resultant VCSFs are detailed in Table V.

TABLE V
VOLTAGE-COST SENSITIVITY FACTOR (1×10^{-6} pu/£)

	MV Feeder 1 End	MV Feeder 2 End	LV Feeder 1 End
MV EES	59.62	5.98	6.29
LV EES	1.03	1.03	355.47
Primary tapchanger	68.79	71.68	77.18
Secondary tapchanger	0.36	0.72	64,212.00

All loads in the case study area are assumed to be constant power loads. Changes in load have been found to have minimal effect on voltage sensitivities [38] therefore the use of offline analysis for calculation of the VCSFs was thought to be valid.

VI. VOLTAGE CONTROL SCHEME EVALUATION

In order to evaluate this voltage control scheme comprehensively, two approaches, IPSA2 simulation and network in the loop emulation, have been adopted.

A detailed model of the case study MV network has been developed in IPSA2 and validated against the field trial results from the CLNR project. Annual load flow, which can be performed by scripting in Python, provides the flexibility of long time evaluation. The long term benefits of the EES and this proposed control scheme can be evaluated by running annual load flow, using the annual SCADA load data and windfarm generation data from Northern Powergrid.

This voltage control scheme is also verified and evaluated with the NIL emulation platform at a smart grid laboratory. With its features of real-time simulation and real LV network, this evaluation approach is able to address many practical issues of the control scheme, such as tolerance of communication delay or loss. Additionally, the three-phase four wire network representation of the NIL system can provide a more realistic representation of LV networks than the three-phase representation in IPSA2.

It should be noted that in this work that an increase in the tap position of a transformer increases the voltage on the secondary side of the transformer.

A. *Baseline of Future Scenario*

The simulation results shown in Fig. 7 and the laboratory emulation results in Fig. 8 and Fig. 9, represent the baseline of the future scenario. In this baseline study, two sustained voltage problems can be observed to occur concurrently on the network. An overvoltage condition on MV Feeder 1, which cannot be easily directly solved by the primary transformer tapchanger, and an overvoltage and voltage imbalance condition on LV feeder 1 which are caused by the high concentrations of unevenly distributed PV generation.

It can be seen from Fig. 7 that during the period where the voltage at the end of MV Feeder 1 is exceeding the upper voltage limit because of the windfarm generation, the voltage at the end of MV Feeder 2 is also close to the lower limit due to the heavy load on this feeder. If a conventional tapchanger based control scheme with remote end measurements is applied, the primary substation tapchanger will be actuated to mitigate the overvoltage at the end of MV Feeder 1, resulting in voltage violation of the lower limit at the end of MV Feeder 2.

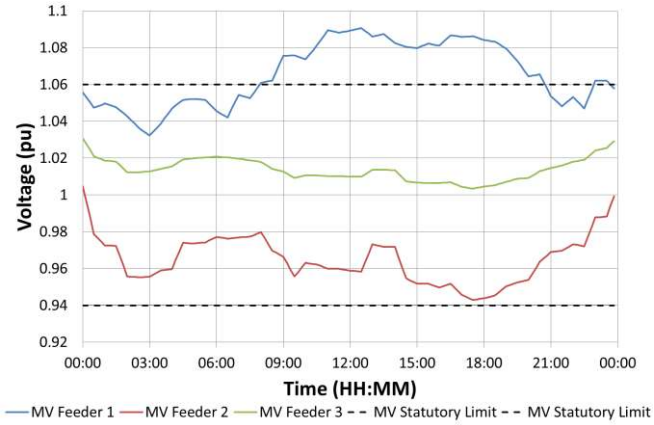

Fig. 7 Voltage profiles at the remote end of MV Feeders - Baseline

Concurrently, in the laboratory, voltage rise and voltage imbalance problems are occurring at the end of LV Feeder 1, where the unbalanced PV cluster is connected, as illustrated in Fig. 8 and Fig. 9.

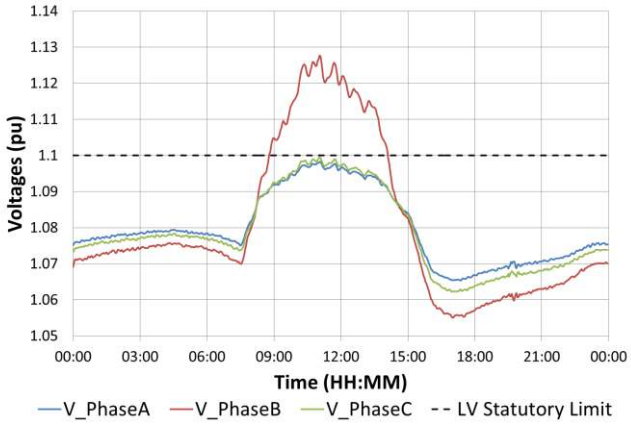

Fig. 8 Three-phase voltage profiles at the end of LV Feeder 1 (Laboratory LV Network) - Baseline

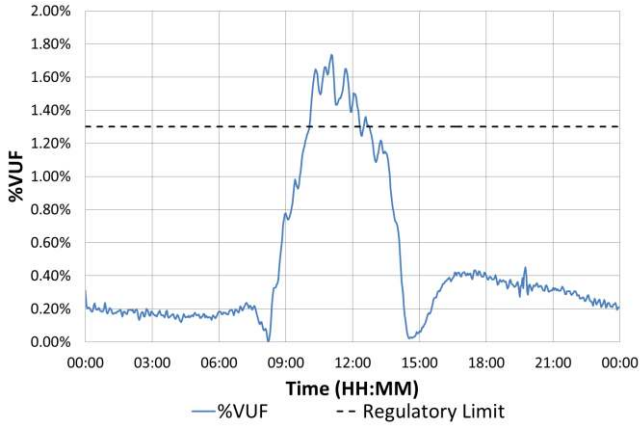

Fig. 9 %VUF at the remote end of LV Feeder 1 (Laboratory LV Network) - Baseline

B. Desktop Implementation and Evaluation of The Control Scheme (Simulation)

The proposed control scheme was realized in Python script in conjunction with the validated network model of the case study network in IPSA2. It should be noted here that in IPSA2, the simulation is three-phase balanced, which means the %VUF is not considered in the simulation approach. The simulation results of the proposed control scheme are shown in Fig. 10, Fig. 11 and Fig. 12. The MV feeder end voltages are illustrated in Fig. 10. The tap position of the primary transformer tapchanger and the power import/export of the MV EES are shown in Fig. 11 and Fig. 12 respectively.

It can be seen from Fig. 10 that at 08:00, the voltage at the end of MV Feeder 1 reaches the MV upper statutory voltage limit. This voltage problem is classified, and all the voltage control solutions are available since the FVDF is less than the threshold. Then the voltage control solution with the largest VCSF is selected, which is the primary tapchanger in this case. The tap position of the primary tap changer against time is shown in Fig. 11. Tap positions in this paper represent the voltage changes at the secondary side of transformers.

At 09:00, the voltage at the end of MV Feeder 1 rises above the MV upper statutory voltage limit. This voltage problem is classified by FVDF being greater than the threshold. As per the control scheme flowchart in Fig. 2, the MV EES is operated to decrease the FVDF. The overvoltage problem is mitigated at the same time when reducing the FVDF.

At 09:10, the voltage at the end of MV Feeder 2 falls below the MV lower statutory voltage limit. This voltage problem is classified by the FVDF being greater than the threshold. As per the control scheme flowchart in Fig. 2 the MV EES is operated to decrease the FVDF. The primary transformer tapchanger is used to increase the voltage at the end of MV Feeder 2 as it has the largest VCSF. It should be noted here that this undervoltage at the end of MV Feeder 2 does not happen in the baseline, due to the windfarm generation. If the windfarm generation reduces or is compensated by the EES, an undervoltage is likely to occur.

At 17:10, a similar undervoltage issue is solved. However, between 17:10 and 19:00, the real power is also required as the MV EES is no longer able to reduce FVDF using reactive power only.

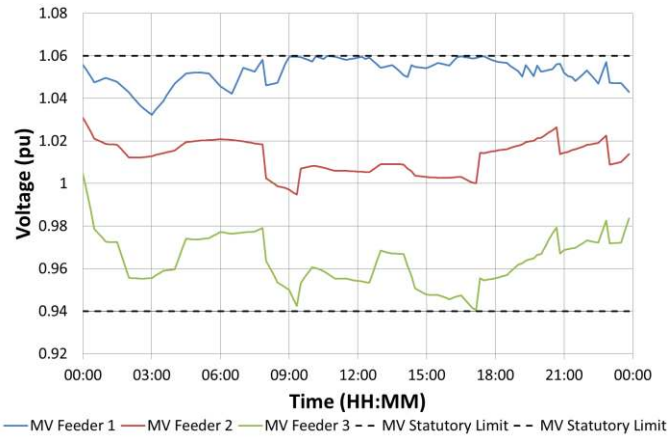

Fig. 10 Voltage profiles at the remote end of MV feeders

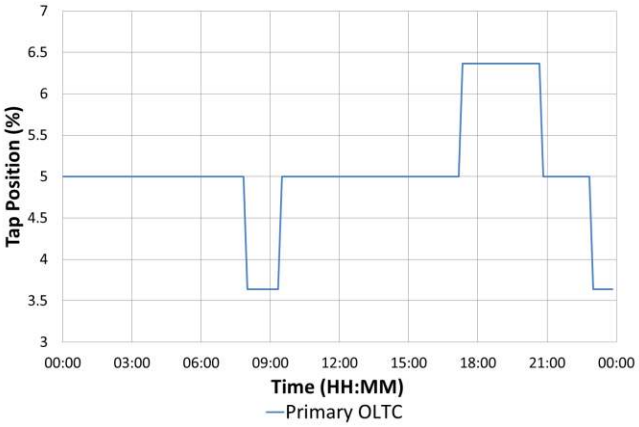

Fig. 11 Tap position of primary transformer tapchanger

Fig. 12 Real and reactive power import of MV EES

In this test case, the target SOC and the initial SOC of the MV EES are both set to 50%. Therefore the VCSF of reactive power is larger than the VCSF of real power in the test case. As a result, reactive power is selected more frequently than real power, which is illustrated in Fig. 12.

At 20:30, the FVDF drops below the threshold. The primary tapchanger lowers the voltage across the feeders, since the primary tapchange has the largest VCSF at this stage, and thus MV EES is not required.

At 22:50, the voltage at the end of MV Feeder 1 reaches the limit again. At this time, the FVDF is smaller than the FVDF threshold and all the voltage control solutions are available. Then the primary tapchanger is selected to control the voltage.

C. Laboratory Implementation and Evaluation of Control Scheme (Emulation and NIL)

1) Smart Grid Laboratory Facility

The network diagram of the smart grid laboratory used in this work is shown in Fig. 13. This laboratory hosts an experimental LV network and a Real Time Digital Simulator (RTDS).

The experimental network includes multiple LCTs and smart grid technologies. Specifically, a PV generation emulator, a wind generation emulator, an EES unit, a Mitsubishi i-MIEV EV, a Mitsubishi Ecodan ASHP, and controllable load banks are connected to the four wire three-phase experimental network.

In addition, the RTDS is connected to the experimental network via a three-phase power amplifier. This arrangement provides the NIL emulation platform, which enables the real experimental LV network to interact with the large scale network model simulated by RTDS in real-time. Furthermore, the system is fully instrumented with precise measurement boards, high-speed data communication network, and human-machine graphical interface.

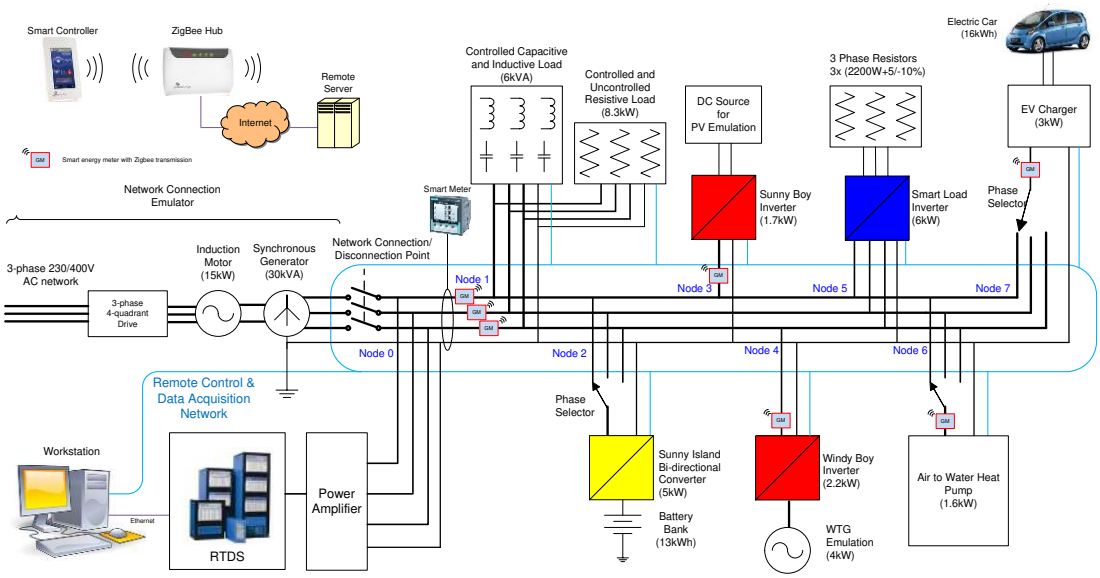

Fig. 13 Smart Grid Laboratory network diagram

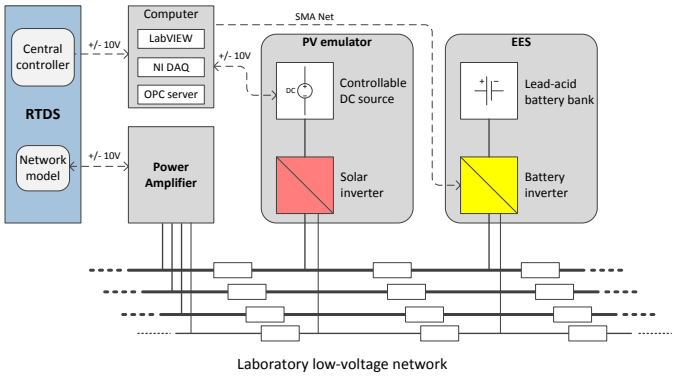

Fig. 14 Layout of NIL emulation of case study

2) Implementation of Network in the Loop Emulation

The layout of the NIL emulation platform for this work is shown in Fig. 14. It consists of the PV emulator, the EES unit, the power amplifier, the LV network, the RTDS and the computer.

To realize the interaction between the network model in RTDS and the real LV network, the RTDS transmits ±10V signals, which reflect the instantaneous voltages of the real-time network model, to the three-phase power amplifier. Then the three-phase power powers up the experimental LV network.

Simultaneously, instantaneous current monitoring signals from the amplifier are fed back to the RTDS. These current signals are used as inputs of the controllable current source in the RTDS model, to reflect the power exchange between the experimental LV network and the network model in RTDS.

To represent the case study network, the simplified MV network and the majority of the PV cluster feeder, LV Feeder 1, are modeled in RSCAD, while the remainder of the PV cluster feeder is emulated in the experimental LV network. In total there are 122 customers on the PV cluster feeder. 120 customers are modeled in RSCAD and the two customers at the end of LV Feeder 1 are emulated by the PV emulator in the experimental LV network. Specifically, the PV emulator comprises of a 1.7kW programmable DC power source and an SMA Sunny Boy inverter. The DC power source is interfaced with LabVIEW from National Instruments, which allows it to model the PV generation profile. The PV generation profile modeled in LabVIEW is then used to control the DC power source to emulate the output of a PV array under varying solar irradiance. Here the PV generation profile represents the net PV generation of two domestic PV customers at the end of LV Feeder 1, which is derived from the PV data and domestic demand data shown in Fig. 6.

The laboratory EES is used to emulate the LV EES located at the end of LV Feeder 1. It consists of a 13kWh lead-acid battery bank and a 5kW SMA Sunny Island single-phase inverter. This unit is controllable in terms of real and reactive power import/export via LabVIEW.

The proposed control scheme has also been developed in RSCAD in conjunction with LabVIEW. The developed control scheme can control the tapchanger in the model simulated in RTDS directly, and it is also able to control the import/export of real and reactive power from the laboratory EES with the help of LabVIEW.

D. Emulation Results

Concurrently with the voltage problems that are observed on the MV network in simulation, described in the previous section, phase B exceeds the statutory voltage limit in the laboratory at approximately 09:00 as illustrated in Fig. 8. This is due to an increase in PV generation in the model and in the laboratory. Three-phase voltages at the end of LV Feeder 1 in the laboratory are shown in Fig. 15. All the voltage control solutions are identified within the set of available solutions since the calculated %VUF and FVDF are within the threshold. The voltage control solution with the largest VCSF, which is the secondary tapchanger in this case, is selected and deployed. The tap position of the secondary tapchanger, which is realized in the RTDS network model, with respect to time is illustrated in Fig. 16.

It can be seen from Fig. 9 that %VUF reaches the regulatory limit at approximately 10:00 due to the uneven distribution of PV generation across the phases on the feeder. The coordinated voltage control scheme classifies this voltage problem. Phase voltage control solutions, which enable phase voltage control, are available for deployment since the %VUF is greater than the threshold. The LV EES is selected and deployed, which has the largest VCSF among all the phase voltage control solutions. The LV EES in the laboratory begins to import real power, charging the battery, to reduce the %VUF under the limit, as shown in Fig. 17 and Fig. 18.

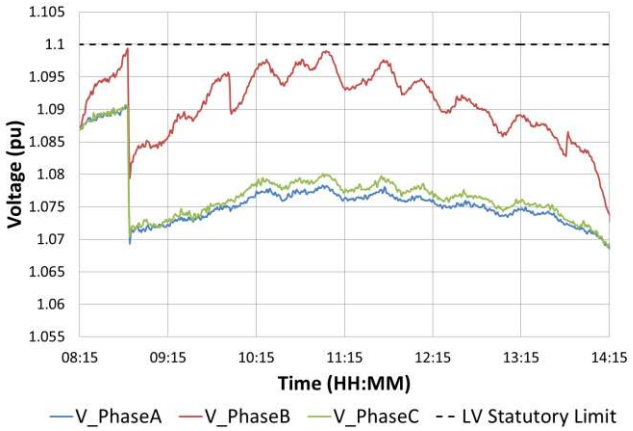

Fig. 15 Three-phase voltage profiles at the remote end of LV Feeder 1 (Laboratory LV Network)

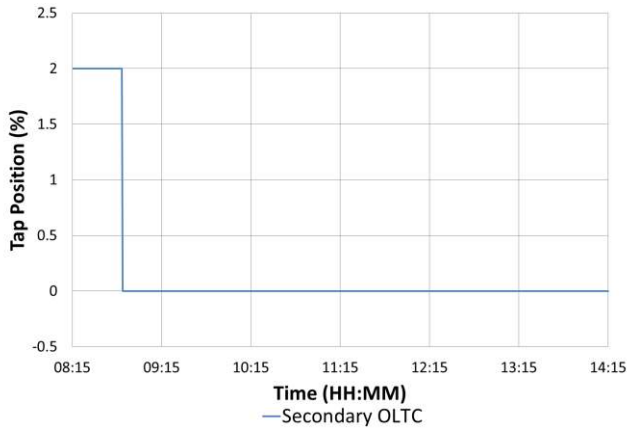

Fig. 16 Tap position of secondary tapchanger (RTDS Network Model)

It should be noted here that in the emulation, only real power of the EES is controlled, since the effect of the reactive power is not significant in the experimental LV network and the VCSF of reactive power is relatively low for this solution. This is due to the low X/R ratio in the experimental LV network.

Fig. 17 %VUF at the remote end of LV Feeder 1 (Laboratory LV Network)

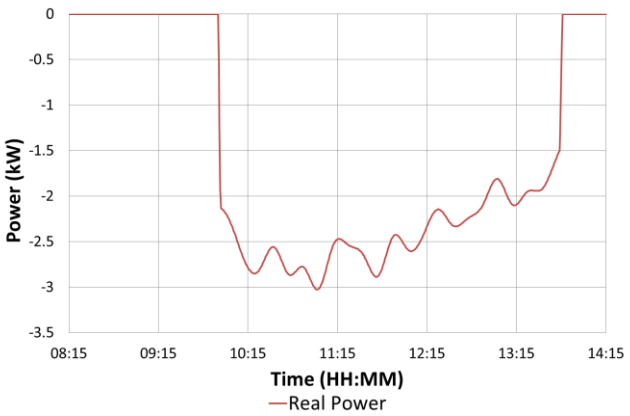

Fig. 18 Real power import of LV EES (Laboratory LV Network)

VII. Conclusions

A coordinated voltage control scheme integrating EES is proposed in this paper for future distribution networks with large, clustered distributions of LCTs, in terms of both feeder and phase location. The scheme is also capable of integrating other FACTS devices by considering them as EES units without real power capability. This proposed control scheme can solve the voltage problems caused by the large, clustered distributions of LCTs, which cannot be addressed by conventional common mode control based voltage control schemes. The proposed scheme can determine and deploy cost optimized solutions for concurrent MV and LV voltage problems, across a range of classifications, simultaneously. In addition, it is shown that integrating EES in the proposed scheme extends its sphere of influence beyond the immediate feeder and increases its value to network operation.

This EES integrated coordinated voltage control scheme is based on a range of network factors and metrics (FVDF, %VUF, VCSF and VSF). FVDF is introduced in this work as a metric for the maximum voltage difference between feeders downstream of a common controlled busbar. FVDF is used in conjunction with %VUF in the proposed control scheme to classify the voltage problems and identify available voltage control solutions. VCSF is derived from voltage sensitivity factors and cost functions for EES and OLTC equipped transformers. VCSF is used to select the cost-optimized voltage control solution, while VSF is utilized to determine the required response of the selected solution.

A case study, in which a credible future scenario is proposed using a validated model of a real GB smart grid trial distribution network, equipped with multiple EES units, OLTC equipped transformers under supervisory control, is used to evaluate the scheme. In this future scenario, clustered concentrations of load and generation LCTs, in terms of both feeder and phase location, are deployed on the case study network. Desktop simulation and laboratory based NIL emulation are jointly conducted to evaluate the control scheme.

The analysis and results from complementary simulation and NIL emulation show that this EES integrated coordinated voltage control scheme can provide cost-optimized voltage control solutions for the distribution networks with highly clustered distributions of load and generation LCTs. This control scheme can solve steady-state voltage excursions and %VUF excursions, which are occurring concurrently at two MV nodes and a LV node in the case study network.

Moreover, it has been found that integrating EES into the coordinated voltage control scheme can increase the value of EES by extending the influence of the EES unit beyond the feeder it is connected, even if it is located towards the remote end of a feeder. This is demonstrated in the case study as the MV feeder connected EES unit is used in collaboration with the primary tapchanger to mitigate a voltage problem on another feeder.

In addition, as the scheme is cognizant of the costs associated with deploying each network solution, it could

reduce costs and increase the operating life of equipment. For example, tapchanger operations are likely to be reduced under this scheme as the cost functions can reflect the age of the devices.

ACKNOWLEDGMENTS

The authors would like to thank Ian Lloyd and Dave Miller from Northern Powergrid, David Roberts from EA Technology and Vincent Thornley from Siemens for their help in accessing data with regards to the case study network and the GUS controller.

VIII. REFERENCES

[1] "International Electrotechnical Vocabulary - Part 601: Generation, transmission and distribution of electricity - General - Low Voltage," in *IEC 60050* vol. 601-01-26, ed, 2009.

[2] "International Electrotechnical Vocabulary - Part 601: Generation, transmission and distribution of electricity - General - Medium Voltage," in *IEC 60050* vol. 601-01-28, ed, 2009.

[3] "The Electricity Safety, Quality and Continuity Regulations," ed, 2002.

[4] C. L. Masters, "Voltage rise: the big issue when connecting embedded generation to long 11 kV overhead lines," *Power Engineering Journal,* vol. 16, pp. 5-12, 2002.

[5] P. F. Lyons, P. C. Taylor, L. M. Cipcigan, P. Trichakis, and A. Wilson, "Small Scale Energy Zones and the Impacts of High Concentrations of Small Scale Embedded Generators," in *Universities Power Engineering Conference, 2006. UPEC '06. Proceedings of the 41st International*, 2006, pp. 128-132.

[6] P. Wang, J. Yi, P. Lyons, D. Liang, P. Taylor, D. Miller*, et al.*, "Customer led network revolution - integrating renewable energy into LV networks using energy storage," *IET Conference Publications,* vol. 2012, p. 223, 2012.

[7] P. Mancarella, G. Chin Kim, and G. Strbac, "Evaluation of the impact of electric heat pumps and distributed CHP on LV networks," in *PowerTech, 2011 IEEE Trondheim*, 2011, pp. 1-7.

[8] T. H. Bradley and A. A. Frank, "Design, demonstrations and sustainability impact assessments for plug-in hybrid electric vehicles," *Renewable and Sustainable Energy Reviews,* vol. 13, p. 115, 2009.

[9] N. S. Wade, P. C. Taylor, P. D. Lang, and P. R. Jones, "Evaluating the benefits of an electrical energy storage system in a future smart grid," *Energy Policy,* vol. 38, pp. 7180-7188, 2010.

[10] C. A. Hill, M. C. Such, C. Dongmei, J. Gonzalez, and W. M. Grady, "Battery Energy Storage for Enabling Integration of Distributed Solar Power Generation," *Smart Grid, IEEE Transactions on,* vol. 3, pp. 850-857, 2012.

[11] M. A. Kashem and G. Ledwich, "Energy requirement for distributed energy resources with battery energy storage for voltage support in three-phase distribution lines," *Electric Power Systems Research,* vol. 77, pp. 10-23, 2007.

[12] B. Hartmann and A. Dan, "Some aspects of distributed generation -- Voltage drop and energy storage," in *PowerTech, 2009 IEEE Bucharest*, 2009, pp. 1-6.

[13] M. Zillmann, Y. Ruifeng, and T. K. Saha, "Regulation of distribution network voltage using dispersed battery storage systems: A case study of a rural network," in *Power and Energy Society General Meeting, 2011 IEEE*, 2011, pp. 1-8.

[14] M. Oshiro, T. Senjyu, A. Yona, N. Urasaki, T. Funabashi, and K. Chul-Hwan, "Optimal operation strategy by battery energy storage systems in distribution system," in *IPEC, 2010 Conference Proceedings*, 2010, pp. 1199-1204.

[15] X. Liu, A. Aichhorn, L. Liu, and H. Li, "Coordinated Control of Distributed Energy Storage System With Tap Changer Transformers for Voltage Rise Mitigation Under High Photovoltaic Penetration," *Smart Grid, IEEE Transactions on,* vol. 3, pp. 897-906, 2012.

[16] P. Wang, J. Yi, P. F. Lyons, D. Liang, P. C. Taylor, D. Miller*, et al.*, "Customer Led Network Revolution - Integrating renewable energy into LV networks using energy storage," in *CIRED Workshop 2012 - Integration of Renewables into the Distribution Grid*, Lisbon, Portugal, 2012.

[17] X.-P. Zhang, C. Rehtanz, and B. Pal, "FACTS-Devices and Applications," in *Flexible AC Transmission Systems: Modelling and Control*, ed: Springer Berlin Heidelberg, 2012, pp. 1-30.

[18] X. Tao, P. C. Taylor, "Voltage Control Techniques for Electrical Distribution Networks Including Distributed Generation," in *The International Federation of Automatic Control*, Seoul, Korea, 2008, pp. 11967-11971.

[19] E. Demirok, D. Sera, R. Teodorescu, P. Rodriguez, and U. Borup, "Clustered PV inverters in LV networks: An overview of impacts and comparison of voltage control strategies," in *Electrical Power & Energy Conference (EPEC), 2009 IEEE*, 2009, pp. 1-6.

[20] A. Augugliaro, L. Dusonchet, S. Favuzza, and E. R. Sanseverino, "Voltage regulation and power losses minimization in automated distribution networks by an evolutionary multiobjective approach," *Power Systems, IEEE Transactions on,* vol. 19, pp. 1516-1527, 2004.

[21] M. E. Elkhatib, R. El-Shatshat, and M. M. A. Salama, "Novel Coordinated Voltage Control for Smart Distribution Networks With DG," *Smart Grid, IEEE Transactions on,* vol. 2, pp. 598-605.

[22] T. Senjyu, Y. Miyazato, A. Yona, N. Urasaki, and T. Funabashi, "Optimal Distribution Voltage Control and Coordination With Distributed Generation," *Power Delivery, IEEE Transactions on,* vol. 23, pp. 1236-1242, 2008.

[23] A. G. Madureira and J. A. Pecas Lopes, "Coordinated voltage support in distribution networks with distributed generation and microgrids," *Renewable Power Generation, IET,* vol. 3, pp. 439-454, 2009.

[24] P. C. Taylor, T. Xu, N. S. Wade, M. Prodanovic, R. Silversides, T. Green*, et al.*, "Distributed voltage control in AuRA-NMS," in *Power and Energy Society General Meeting, 2010 IEEE*, pp. 1-7.

[25] D. Villacci, G. Bontempi, and A. Vaccaro, "An adaptive local learning-based methodology for voltage regulation in distribution networks with dispersed generation," *Power Systems, IEEE Transactions on,* vol. 21, pp. 1131-1140, 2006.

[26] P. Trichakis, P. C. Taylor, L. M. Cipcigan, P. F. Lyons, R. Hair, and T. Ma, "An Investigation of Voltage Unbalance in Low Voltage Distribution Networks with High Levels of SSEG," in *Universities Power Engineering Conference, 2006. UPEC '06. Proceedings of the 41st International*, 2006, pp. 182-186.

[27] P. Trichakis, P. C. Taylor, P. F. Lyons, and R. Hair, "Predicting the technical impacts of high levels of small-scale embedded generators on low-voltage networks," *Renewable Power Generation, IET,* vol. 2, pp. 249-262, 2008.

[28] A. von Jouanne and B. Banerjee, "Assessment of voltage unbalance," *Power Delivery, IEEE Transactions on,* vol. 16, pp. 782-790, 2001.

[29] "Engineering Recommendation P29: Planning limits for voltage unbalance in the United Kingdom," The Electricity Association, London, UK1990.

[30] "EN 50160: Voltage characteristics of electricity supplied by public distribution systems," ed. Brussels, Belgium: CENELEC, 1999.

[31] K. Jong-Gyeum, L. Eun-Woong, L. Dong-Ju, and L. Jong-Han, "Comparison of voltage unbalance factor by line and phase voltage," in *Electrical Machines and Systems, 2005. ICEMS 2005. Proceedings of the Eighth International Conference on*, 2005, pp. 1998-2001 Vol. 3.

[32] B. Werther, J. Schmiesing, A. Becker, and E.-A. Wehrmann, "Voltage control in low voltage systems with controlled low voltage transformer (CLVT)," in *Integration of Renewables into the Distribution Grid, CIRED 2012 Workshop*, 2012, pp. 1-4.

[33] A. Keane, Q. Zhou, J. W. Bialek, and M. O'Malley, "Planning and operating non-firm distributed generation," *Renewable Power Generation, IET,* vol. 3, pp. 455-464, 2009.

[34] S. Abu-Sharkh, R. Arnold, J. Kohler, R. Li, T. Markvart, J. Ross, *et al.*, "Can microgrids make a major contribution to UK energy supply?," *Renewable & Sustainable Energy Reviews,* vol. 10, pp. 78-127, 2006.

[35] A. A. Sousa, G. L. Torres, and C. A. Canizares, "Robust Optimal Power Flow Solution Using Trust Region and Interior-Point Methods," *Power Systems, IEEE Transactions on,* vol. 26, pp. 487-499, 2011.

[36] E. Veldman, M. Gibescu, H. Slootweg, and W. L. Kling, "Impact of electrification of residential heating on loading of distribution networks," in *PowerTech, 2011 IEEE Trondheim*, 2011, pp. 1-7.

[37] DECC/OFGEM. (2012, 3rd August). *Smart Grid Forum*. Available: http://www.ofgem.gov.uk/Networks/SGF/Pages/SGF.aspx

[38] M. A. Kashem and G. Ledwich, "Multiple Distributed Generators for Distribution Feeder Voltage Support," *Energy Conversion, IEEE Transactions on,* vol. 20, pp. 676-684, 2005.

Pengfei Wang (S'11) received his B.Eng degree from Shanghai Jiao Tong University, Shanghai, China in 2007, and M.Sc. degree from TU Darrnstadt University, Darmstadt; Germany in 2010, both in electrical power engineering. He worked in ALSTOM Grid, Stafford, UK, as a certification engineering on protection relays after he got his mater degree.

He is currently pursuing a Ph.D. at Newcastle University in the field of power systems engineering. His research interests include low carbon technologies integration and coordinated voltage control in distribution networks.

Daniel H. Liang received his B.Eng degree and M. Eng degree in electrical engineering in 2000 and 2003 respectively and his PhD degree in 2008 from Nanyang Technological University, Singapore. From 2006 to 2011 he worked in industries and university at Singapore.

He is currently working at Durham University, UK as a senior smart grid engineer. His research interests include smart grid experimental design and voltage and powerflow management of smart grids.

Pádraig F. Lyons (M' 10) received his B.E. degree in electrical and electronic engineering and an MEng.Sc degree in electrical engineering from University College Cork, Cork, Ireland in 1999 and 2002 respectively and his Ph.D. degree from Durham University, Durham, UK, 2010.

He is currently a senior smart grids researcher at Newcastle University. He also has industrial experience at ESBI, Ireland and at TNEI Services Ltd., UK. His research interests include active network management (ANM), smart grids and experimental design and analysis for smart grids.

Dr Lyons is a chartered engineer.

Jialiang Yi (S'12) received the M.Sc. degree from Southampton University in sustainable energy technology, Southampton, UK in 2011.

He is currently pursuing a Ph.D. at Newcastle University in the field of power systems engineering. His research interests include electrical energy storage systems and demand side response in distribution networks.

Peter J. Davison received B.Eng. and M.Sc. degrees from Durham University, UK in 2010 and 2011 respectively.

He is currently studying for a Ph.D. in smart grids at Newcastle University. His research interests include real time thermal ratings and domestic load modeling.

Philip C. Taylor (SM' 12) received an Engineering Doctorate in the field of intelligent demand side management techniques from the University of Manchester Institute of Science and Technology (UMIST), Manchester, UK, 2001.

He has significant industrial experience as an electrical engineer including a period working in the transmission and distribution projects team at GEC Alstom and was Research and Development Director at Econnect (Now Senergy Econnect), a consultancy firm specializing in the grid integration of renewable energy.

Professor Taylor is currently the Director of the Newcastle Institute for Research on Sustainability (NIReS) and Professor of Electrical Power Systems at the School of Electrical and Electronic Engineering, Newcastle University. Professor Taylor is a member of the EPSRC Peer Review College and the CIGRE working group C6.11, "Development and Operation of Active Distribution Networks".